THE JOURNAL OF PHYSICAL CHEMISTRY C

Article

pubs.acs.org/JPCC

Nuclear Magnetic Resonance Study of Atomic Motion in $A_2B_{12}H_{12}$ (A = Na, K, Rb, Cs): Anion Reorientations and Na^+ Mobility

Alexander V. Skripov,*[,†] Olga A. Babanova,[†] Alexei V. Soloninin,[†] Vitalie Stavila,[‡] Nina Verdal,[§,∥] Terrence J. Udovic,[§] and John J. Rush[§,∥]

[†]Institute of Metal Physics, Ural Division of the Russian Academy of Sciences, S. Kovalevskoi 18, Ekaterinburg 620990, Russia

[‡]Sandia National Laboratories, Livermore, California 94551-0969, United States

[§]NIST Center for Neutron Research, National Institute of Standards and Technology, 100 Bureau Drive, Gaithersburg, Maryland 20899-6102, United States

[∥]Department of Materials Science and Engineering, University of Maryland, College Park, Maryland 20742-2115, United States

ABSTRACT: To study the reorientational motion of icosahedral $[B_{12}H_{12}]^{2-}$ anions in $A_2B_{12}H_{12}$ (A = Na, K, Rb, Cs) and the translational diffusion of Na^+ cations in $Na_2B_{12}H_{12}$, we have measured the ^1H, ^{11}B, and ^{23}Na NMR spectra and spin–lattice relaxation rates in these compounds over the temperature range of 170–580 K. For cubic compounds $K_2B_{12}H_{12}$, $Rb_2B_{12}H_{12}$, and $Cs_2B_{12}H_{12}$, the measured ^1H and ^{11}B spin–lattice relaxation rates are governed by thermally activated reorientations of the $[B_{12}H_{12}]^{2-}$ anions. The activation energy of this reorientational motion is found to decrease with increasing cation radius, changing from 800 meV for $K_2B_{12}H_{12}$ to 549 meV for $Rb_2B_{12}H_{12}$ and 427 meV for $Cs_2B_{12}H_{12}$. For $Na_2B_{12}H_{12}$, the first-order transition from the low-temperature monoclinic to the high-temperature cubic phase near 520 K is accompanied by a 2 orders of magnitude increase in the reorientational jump rate, and the corresponding activation energy changes from 770 meV for the low-T phase to 270 meV for the high-T phase. Measurements of the ^{23}Na NMR spectra and spin–lattice relaxation rates show that the transition from the low-T to the high-T phase of $Na_2B_{12}H_{12}$ is also accompanied by the onset of the fast translational diffusion of Na^+ ions. Just above the transition point, the lower limit of the Na^+ jump rate estimated from the ^{23}Na spin–lattice relaxation data is 2×10^8 s^{-1}, and the corresponding activation energy for Na^+ diffusion is about 410 meV.

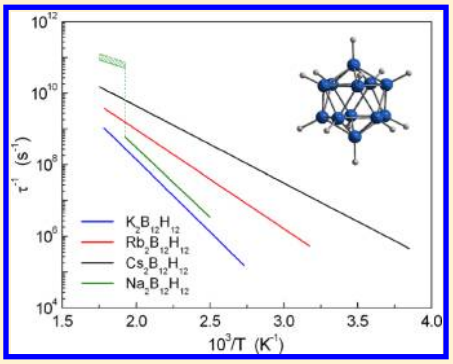

INTRODUCTION

Alkali-metal (A) dodecahydro-*closo*-dodecaborates $A_2B_{12}H_{12}$ are ionically bonded salts consisting of alkali-metal A^+ cations and icosahedral $[B_{12}H_{12}]^{2-}$ anions. The inherently high stability and orientational mobility of the anions and the relatively large anion/cation size ratios lead to intriguing physical properties, including high-temperature order–disorder phase transitions concomitant with potentially enhanced cationic mobilities.[1−3] In addition to their interest from a fundamental viewpoint, the dodecahydro-*closo*-dodecaborate salts, particularly the lighter Li, Na, and K analogues, have received recent attention, since they are energetically favorable intermediate compounds[2−7] in the decomposition of the corresponding borohydrides ABH_4, a promising class of hydrogen-storage materials. The persistence of these highly stable salts, once they are formed, is believed to be partly responsible for the poor hydrogen cycling performance of the borohydrides. Room-temperature crystal structures of the $A_2B_{12}H_{12}$ compounds are cubic (space group $Fm\bar{3}$) for A = K, Rb, and Cs,[8,9] monoclinic ($P2_1/n$) for $Na_2B_{12}H_{12}$,[10] and cubic ($Pa\bar{3}$) for $Li_2B_{12}H_{12}$.[11] All these compounds are known (either directly via diffraction or indirectly via differential scanning calorimetry) to undergo first-order or second-order structural phase transitions at high temperatures (~628, 520, 811, 742, and 529 K for A = Li, Na, K, Rb, and Cs, respectively[1,3]) before they decompose. These phase transitions involve an orientational disordering of the $[B_{12}H_{12}]^{2-}$ anions. Fundamental information on the reorientational dynamics of $[B_{12}H_{12}]^{2-}$ anions for various $A_2B_{12}H_{12}$ compounds may ultimately help to better understand the nature of these disorder-driven phase transitions. Moreover, at least for the lighter Li and Na analogues, the high-temperature disordered $A_2B_{12}H_{12}$ phases are stable at the temperatures of the borohydride decomposition and reformation. Thus, these phases need to be considered in any theoretical analysis of the borohydride reversibility.[2]

Studies of the ^{11}B nuclear magnetic resonance (NMR) spectra[12] for $K_2B_{12}H_{12}$, $Rb_2B_{12}H_{12}$, and $Cs_2B_{12}H_{12}$ have shown that the $[B_{12}H_{12}]^{2-}$ anions (Figure 1) in these salts participate in the fast reorientational motion, and the jump rate τ^{-1} of this motion at a given temperature increases with increasing cation radius. For the salt with the largest alkali-metal cation, $Cs_2B_{12}H_{12}$, the reorientational motion of the $B_{12}H_{12}$ groups

Received: October 29, 2013
Revised: November 22, 2013
Published: November 22, 2013

   dx.doi.org/10.1021/jp4106585 | J. Phys. Chem. C 2013, 117, 25961−25968

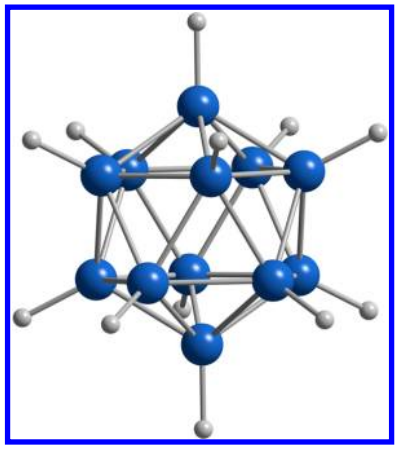

Figure 1. Schematic view of the icosahedral $[B_{12}H_{12}]^{2-}$ anion. Large blue spheres: B atoms; small gray spheres: H atoms.

has also been studied by quasielastic neutron scattering (QENS).[13] The observed changes in the elastic incoherent structure factor (EISF) for $Cs_2B_{12}H_{12}$ over the temperature range 430−530 K suggest a possibility of changes in the mechanism of reorientations in this range.[13] It should be noted that both NMR spectral measurements and QENS measurements can trace the atomic jump rate variations over rather limited dynamic ranges (usually, not exceeding 2 orders of magnitude). In contrast, NMR measurements of the nuclear spin−lattice relaxation rates can trace the changes in τ^{-1} over much wider dynamic ranges (up to 8 orders of magnitude for some alkali-metal borohydrides.)[14,15] Such a wide dynamic range is expected to result in the high accuracy of the measured activation energies for the reorientational motion. Measurements of the nuclear spin−lattice relaxation rates at different resonance frequencies (i.e., at different magnetic fields) can also be used to search for a distribution of τ^{-1} values[16] or a coexistence of several types of jump motion with different rates.[17,18] The aim of the present work is to investigate the parameters of the reorientational motion of $[B_{12}H_{12}]^{2-}$ anions in four $A_2B_{12}H_{12}$ compounds (A = Na, K, Rb, and Cs) using the ^1H and ^{11}B spin−lattice relaxation rate measurements over the wide temperature range (250−580 K) and at different resonance frequencies. We have also studied the effects of the first-order structural phase transition in $Na_2B_{12}H_{12}$ on the reorientational motion of $[B_{12}H_{12}]^{2-}$ anions and the translational mobility of Na^+ cations, which may be affected by any changes in the rotational mobility of their anion neighbors.

EXPERIMENTAL METHODS

The preparation of the $A_2B_{12}H_{12}$ samples was analogous to that described in refs 8, 10, and 19. Prior to experiments, any residual water was removed from the samples by annealing them in vacuum at 473−523 K; subsequently, the samples were flame-sealed in glass tubes. ^1H, ^{11}B, and ^{23}Na NMR measurements were performed on a pulse spectrometer with quadrature phase detection at the frequencies $\omega/2\pi$ = 14 and 23.8 MHz for ^1H, 14 and 28 MHz for ^{11}B, and 23 MHz for ^{23}Na. The magnetic field was provided by a 2.1 T iron-core Bruker magnet. A home-built multinuclear continuous-wave NMR magnetometer working in the range 0.32−2.15 T was used for field stabilization. For rf pulse generation, we used a home-built computer-controlled pulse programmer, the PTS frequency synthesizer (Programmed Test Sources, Inc.[20]), and a 1 kW Kalmus wideband pulse amplifier. Typical values of the $\pi/2$ pulse length were 2−3 μs for all nuclei studied. For the measurements at $T \leq 470$ K, a probehead with the sample was placed into an Oxford Instruments CF1200 continuous-flow cryostat using nitrogen as a cooling agent. The sample temperature, monitored by a chromel−(Au−Fe) thermocouple, was stable to ±0.1 K. Measurements in the temperature range 470−580 K were performed using a furnace probehead; for this setup, the sample temperature, monitored by a copper−constantan thermocouple, was stable to ±0.5 K. The nuclear spin−lattice relaxation rates were measured using the saturation−recovery method. NMR spectra were recorded by Fourier transforming the solid echo signals (pulse sequence $\pi/2_x-t-\pi/2_y$). It should be noted that for all figures in this paper standard uncertainties are commensurate with the scatter in the data.

RESULTS AND DISCUSSION

Cubic $K_2B_{12}H_{12}$, $Rb_2B_{12}H_{12}$, and $Cs_2B_{12}H_{12}$. The temperature dependences of the proton spin−lattice relaxation rates R_1^H measured at two resonance frequencies $\omega/2\pi$ for $K_2B_{12}H_{12}$, $Rb_2B_{12}H_{12}$, and $Cs_2B_{12}H_{12}$ are shown in Figures 2 and 3.

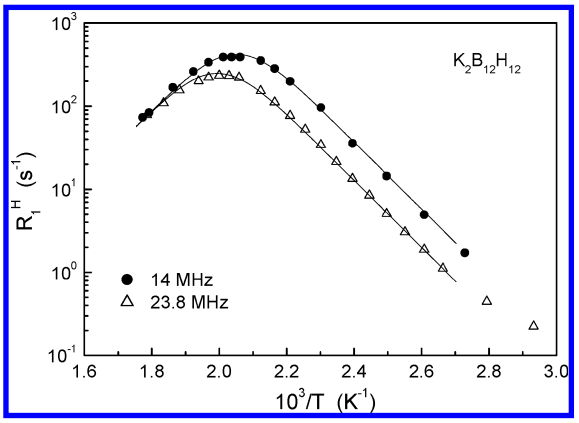

Figure 2. Proton spin−lattice relaxation rates measured at 14 and 23.8 MHz for $K_2B_{12}H_{12}$ as functions of the inverse temperature. The solid lines show the simultaneous fit of the standard model to the data.

General features of the observed behavior of R_1^H in these compounds are typical of the relaxation mechanism due to

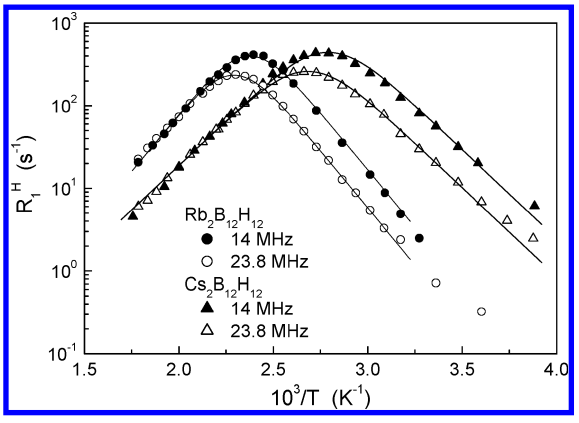

Figure 3. Proton spin−lattice relaxation rates measured at 14 and 23.8 MHz for $Rb_2B_{12}H_{12}$ and $Cs_2B_{12}H_{12}$ as functions of the inverse temperature. The solid lines show the simultaneous fits of the standard model to the data.

dx.doi.org/10.1021/jp4106585 | J. Phys. Chem. C 2013, 117, 25961−25968

nuclear dipole−dipole interaction modulated by thermally activated atomic motion.[21] In our case, the motion can be identified as reorientations of the icosahedral $[B_{12}H_{12}]^{2-}$ anions;[12] this is supported by the behavior of the width of the ^{1}H NMR spectra, to be discussed below.

As can be seen from Figures 2 and 3, for each of the studied compounds, $R_1^H(T)$ exhibits the frequency-dependent peak. This peak is expected to occur at the temperature at which the reorientation jump rate τ^{-1} becomes nearly equal to ω.[21] Thus, the position of the $R_1^H(T)$ peak may be used to compare the jump rates in different compounds: for compounds with faster motion, the $R_1^H(T)$ peak should be observed at lower temperatures. At $\omega/2\pi$ = 14 MHz, we observe the $R_1^H(T)$ maxima at 490 K for $K_2B_{12}H_{12}$, at 417 K for $Rb_2B_{12}H_{12}$, and at 365 K for $Cs_2B_{12}H_{12}$. These results indicate that the rate of the $[B_{12}H_{12}]^{2-}$ reorientations increases with increasing cation radius, in qualitative agreement with previous conclusions.[12]

The standard theory of nuclear spin−lattice relaxation due to the motionally modulated dipole−dipole interaction[21] predicts that in the limit of slow motion ($\omega\tau \gg 1$) R_1^H is proportional to $\omega^{-2}\tau^{-1}$, and in the limit of fast motion ($\omega\tau \ll 1$), R_1^H is proportional to τ being frequency-independent. If the temperature dependence of the jump rate τ^{-1} follows the Arrhenius law

$$\tau^{-1} = \tau_0^{-1} \exp\left(\frac{-E_a}{k_B T}\right) \quad (1)$$

with the activation energy E_a, the plot of ln R_1^H versus T^{-1} is expected to be linear in the limits of both slow and fast motion with the slopes of $-E_a/k_B$ and E_a/k_B, respectively. Our experimental R_1^H data (Figures 2 and 3) are consistent with these predictions. For all the studied compounds, we have not found any signs of distributions of the jump rates. Indeed, the presence of a distribution of τ^{-1} values would have led[16] to the difference between the high-T and low-T slopes of the ln R_1^H versus T^{-1} plot and to the weakened (weaker than ω^{-2}) frequency dependence of R_1^H at the low-T slope; such features are not observed in our experiments. Thus, for parametrization of the $R_1^H(T)$ results we have used the standard theory[21] and eq 1; the same approach was earlier employed for the reorientational motion in alkali-metal borohydrides.[15,22] The fit parameters are the activation energy E_a, the pre-exponential factor τ_0 in the Arrhenius law, and the amplitude parameter determined by the strength of the fluctuating part of dipole−dipole interaction. These parameters have been varied to find the best fit to the $R_1^H(T)$ data at the two frequencies simultaneously. The results of the simultaneous fit are shown by solid curves in Figures 2 and 3. The corresponding motional fit parameters are $\tau_0 = (6.0 \pm 0.5) \times 10^{-17}$ s and E_a = 800 ± 8 meV for $K_2B_{12}H_{12}$, $\tau_0 = (3.1 \pm 0.7) \times 10^{-15}$ s and E_a = 549 ± 5 meV for $Rb_2B_{12}H_{12}$, and $\tau_0 = (1.1 \pm 0.4) \times 10^{-14}$ s and E_a = 427 ± 4 meV for $Cs_2B_{12}H_{12}$. The temperature dependences of the jump rates τ^{-1} resulting from the fits are shown in Figure 4 in the form of Arrhenius plots. The temperature ranges of the lines in this figure correspond to the actual ranges of the fitted $R_1^H(T)$ data.

As can be seen from Figure 4, the proton spin−lattice relaxation measurements allow us to trace the changes in the jump rate of reorientations in $K_2B_{12}H_{12}$, $Rb_2B_{12}H_{12}$, and $Cs_2B_{12}H_{12}$ over the range of at least 4 orders of magnitude. Such a wide dynamic range is expected to lead to high accuracy of the E_a values derived from the $R_1^H(T)$ data. In Table 1, the values of the activation energies obtained from our proton spin−lattice relaxation measurements are compared to the corresponding results from previous works.

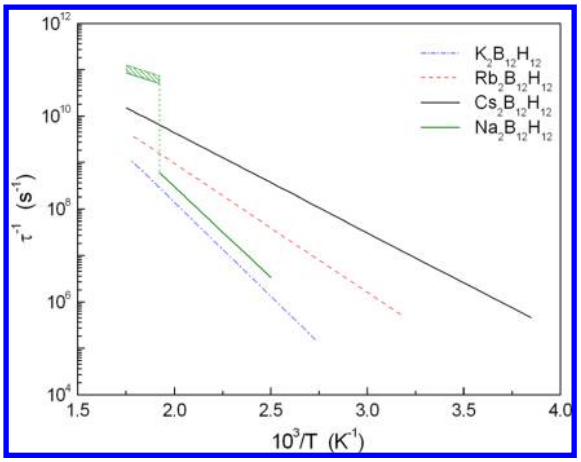

Figure 4. Temperature dependences of the jump rates of $[B_{12}H_{12}]^{2-}$ reorientations, as derived from the fits to the proton spin−lattice relaxation data for $K_2B_{12}H_{12}$, $Rb_2B_{12}H_{12}$, $Cs_2B_{12}H_{12}$, and $Na_2B_{12}H_{12}$. The temperature ranges of the lines correspond to the actual temperature ranges of the fitted relaxation rate data. The shaded green area reflects the approximate character of the jump rates obtained for the high-temperature phase of $Na_2B_{12}H_{12}$.

Table 1. Activation Energies for $[B_{12}H_{12}]^{2-}$ Reorientations in $A_2B_{12}H_{12}$ Compounds, As Derived from NMR and QENS Experiments[a]

compound	E_a (meV)	T range (K)	method	ref
$K_2B_{12}H_{12}$	1070 (54)	~270−370	^{11}B NMR spectra	12
	800 (8)	366−564	^{1}H spin−lattice relaxation	this work
$Rb_2B_{12}H_{12}$	910 (46)	~220−340	^{11}B NMR spectra	12
	549 (5)	315−560	^{1}H spin−lattice relaxation	this work
$Cs_2B_{12}H_{12}$	600 (30)	~180−300	^{11}B NMR spectra	12
	333 (15)	430−530	QENS	13
	427 (4)	260−570	^{1}H spin−lattice relaxation	this work
$Na_2B_{12}H_{12}$ (LT phase)	770 (20)	400−520	^{1}H spin−lattice relaxation	this work
$Na_2B_{12}H_{12}$ (HT phase)	270 (40)	523−570	^{1}H spin−lattice relaxation	this work

[a]Uncertainties in the last digit are given in parentheses.

The values of E_a obtained from changes in the ^{11}B NMR line width in $K_2B_{12}H_{12}$, $Rb_2B_{12}H_{12}$, and $Cs_2B_{12}H_{12}$ in ref 12 appear to be considerably overestimated. An additional indication of overestimated E_a values in ref 12 is the unreasonably small values of the pre-exponential factor τ_0 derived by Tiritiris et al.[12] (5.9×10^{-21} s for $K_2B_{12}H_{12}$ and 7.1×10^{-23} s for $Rb_2B_{12}H_{12}$). Such small values of τ_0 are difficult to justify. Generally, temperature dependences of NMR spectra are not suitable for precise determination of the activation energies of atomic motions; in this respect, spin−lattice relaxation rates are known to be more effective.[23] On the other hand, the value of E_a for $Cs_2B_{12}H_{12}$ derived from QENS measurements[13] is lower than that from the present proton spin−lattice relaxation measurements. This discrepancy may be due to the very limited

dx.doi.org/10.1021/jp4106585 | J. Phys. Chem. C 2013, 117, 25961−25968

dynamic range of the backscattering QENS experiments[13] (the corresponding jump rate changed only by a factor of 7).

Figure 5 shows the temperature dependences of the full width at half-maximum, $\Delta\nu_H$, of the ^{1}H NMR spectra for

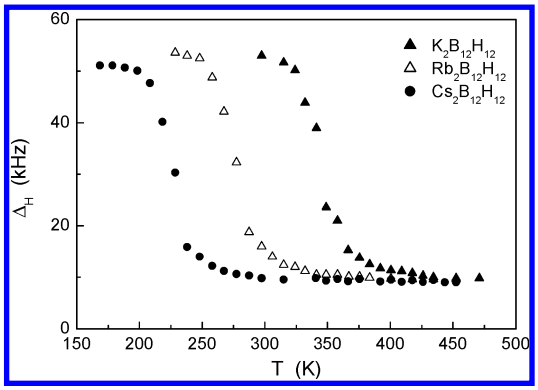

Figure 5. Temperature dependences of the widths (full widths at half-maximum) of the ^{1}H NMR lines measured at 23.8 MHz for $K_2B_{12}H_{12}$, $Rb_2B_{12}H_{12}$, and $Cs_2B_{12}H_{12}$.

$K_2B_{12}H_{12}$, $Rb_2B_{12}H_{12}$, and $Cs_2B_{12}H_{12}$. For all these compounds, the observed line narrowing indicates the excitation of H jump motion on the frequency scale of the order of 10^5 s^{-1}. As the cation radius increases, the region of the sharp drop in $\Delta\nu_H$ shifts to lower temperatures; this indicates that the motion becomes faster, in qualitative agreement with the proton spin–lattice relaxation results. For all the studied compounds, above the region of the sharp drop the proton line width stops to decrease, being nearly constant up to the highest temperature of our measurements. The substantial plateau value of $\Delta\nu_H$ (~10 kHz) indicates that the motion responsible for the observed line narrowing is indeed localized (as expected for the reorientational motion), since such a motion leads to only partial averaging of dipole–dipole interactions between nuclear spins. In the studied temperature range, we have not found any signs of translational diffusion of H-containing species on the frequency scale of 10^5 s^{-1}.

General features of the temperature dependences of the measured ^{11}B spin–lattice relaxation rates R_1^B for $A_2B_{12}H_{12}$ (A = K, Rb, and Cs) are similar to those of the proton spin–lattice relaxation rates for the corresponding compounds. In particular, for each of the three compounds, the ^{11}B spin–lattice relaxation rate exhibits a frequency-dependent peak at nearly the same temperature as the ^{1}H relaxation rate. As an example of the data, Figure 6 shows the behavior of the ^{11}B spin–lattice relaxation rates measured at two resonance frequencies for $Rb_2B_{12}H_{12}$ and $Cs_2B_{12}H_{12}$. It is natural to assume that the $R_1^B(T)$ peak originates from the same reorientational motion of $[B_{12}H_{12}]^{2-}$ anions as the $R_1^H(T)$ peak. However, in contrast to the case of alkali-metal borohydrides,[15,22] the amplitude of $R_1^B(T)$ peak for $A_2B_{12}H_{12}$ compounds is much higher than the amplitude of the corresponding $R_1^H(T)$ peak. For example, for $Rb_2B_{12}H_{12}$ at $\omega/2\pi$ = 14 MHz the maximum R_1^B value is 5320 s^{-1}, while the maximum R_1^H value is 415 s^{-1}. This feature suggests that the ^{11}B spin–lattice relaxation rate in $A_2B_{12}H_{12}$ compounds is dominated by the quadrupole mechanism related to electric-field-gradient (EFG) fluctuations at nuclear sites. For alkali-metal borohydrides, reorientations of a BH_4 tetrahedron do not cause any strong EFG fluctuations at the central B site, so that the ^{11}B spin–lattice relaxation is dominated by the ^{11}B–^{1}H dipole–dipole interaction, and the maximum R_1^B values

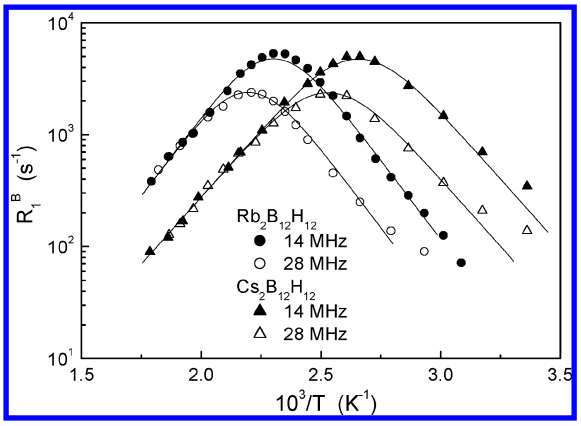

Figure 6. ^{11}B spin–lattice relaxation rates measured at 14 and 28 MHz for $Rb_2B_{12}H_{12}$ and $Cs_2B_{12}H_{12}$ as functions of the inverse temperature. The solid lines show the simultaneous fits of the model based on eqs 2 and 1 to the data.

appear to be close to the maximum R_1^H values.[15,22] In the case of $A_2B_{12}H_{12}$ compounds, any rotation of the $B_{12}H_{12}$ group (Figure 1) is expected to change the angle between the principal axis of the EFG tensor for most of B sites and the magnetic field direction, providing the effective quadrupole relaxation mechanism. We have not found any significant deviations from a single-exponential recovery of the ^{11}B nuclear magnetization in the regions of the $R_1^B(T)$ peaks.

The simplest approach to describe the motionally induced quadrupole contribution to the spin–lattice relaxation rate is based on the expression

$$R_1^B = \frac{M_Q}{\omega}\left[\frac{y}{1+y^2} + \frac{4y}{1+4y^2}\right] \quad (2)$$

where $y = \omega\tau$, and eq 1. Here the amplitude factor M_Q is proportional to the square of the electric quadrupole moment of ^{11}B and the mean square of the fluctuating part of EFG at ^{11}B sites due to reorientations. The amplitude factor and the motional parameters (E_a and τ_0) have been varied to find the best fit of eqs 2 and 1 to the $R_1^B(T)$ data at two resonance frequencies simultaneously. The results of such simultaneous fits for $Rb_2B_{12}H_{12}$ and $Cs_2B_{12}H_{12}$ are shown by solid curves in Figure 6. For $K_2B_{12}H_{12}$ and $Rb_2B_{12}H_{12}$, the motional parameters resulting from these fits are very close to the corresponding parameters derived from the ^{1}H spin–lattice relaxation data. In particular, the activation energies for reorientational motion obtained from the $R_1^B(T)$ fits (820 ± 15 meV for $K_2B_{12}H_{12}$ and 560 ± 10 meV for $Rb_2B_{12}H_{12}$) agree within experimental uncertainties with the corresponding values from the $R_1^H(T)$ fits (see Table 1). For $Cs_2B_{12}H_{12}$, the activation energy from the $R_1^B(T)$ fit (477 ± 8 meV) is 12% higher than the corresponding value from the $R_1^H(T)$ fit. The nature of this discrepancy is not yet understood. It should be noted that we have not found any anomalies in the behavior of the ^{1}H and ^{11}B spin–lattice relaxation rates near the second-order phase transition[1] to the reorientationally disordered state of $Cs_2B_{12}H_{12}$ at 529 K.

Monoclinic $Na_2B_{12}H_{12}$ and the Effects of the Phase Transition. The proton spin–lattice relaxation rates for $Na_2B_{12}H_{12}$ measured at two resonance frequencies are shown in Figure 7. At T < 520 K, the behavior of the $R_1^H(T)$ for $Na_2B_{12}H_{12}$ resembles that for the other $A_2B_{12}H_{12}$ (A = K, Rb, Cs) compounds. The relaxation rate maximum for $Na_2B_{12}H_{12}$

dx.doi.org/10.1021/jp4106585 | J. Phys. Chem. C 2013, 117, 25961–25968

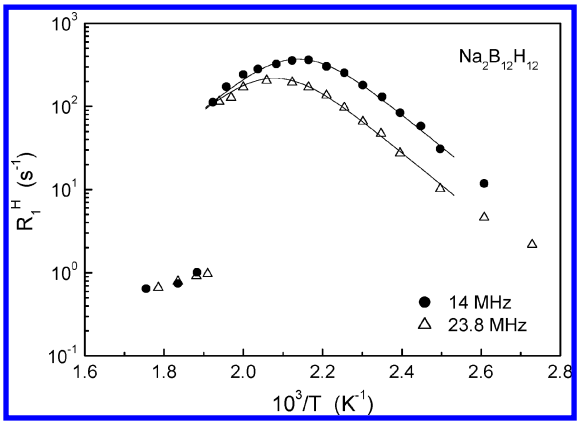

Figure 7. Proton spin−lattice relaxation rates measured at 14 and 23.8 MHz for $Na_2B_{12}H_{12}$ as functions of the inverse temperature. The solid lines show the simultaneous fit of the standard model to the data for the low-temperature phase.

at $\omega/2\pi$ = 14 MHz is observed near 465 K. Using the same approach as for the cubic $A_2B_{12}H_{12}$ (A = K, Rb, Cs) compounds, we have fitted the standard model[21] to the $R_1^H(T)$ data for $Na_2B_{12}H_{12}$ over the range of 400−520 K at two resonance frequencies simultaneously. The results of such a simultaneous fit are shown by the solid lines in Figure 7. The motional parameters derived from this fit are $\tau_0 = (5.7 \pm 2.6) \times 10^{-17}$ s and E_a = 770 ± 20 meV. As in the case of the other $A_2B_{12}H_{12}$ compounds, we have not found any signs of a distribution of the jump rates for $Na_2B_{12}H_{12}$. The Arrhenius plot of $\tau^{-1}(T)$ resulting from the fit for $Na_2B_{12}H_{12}$ is included in Figure 4.

The dramatic decrease in the proton spin−lattice relaxation rate observed near 520 K (Figure 7) can be attributed to the first-order phase transition from the low-temperature monoclinic to the high-temperature cubic phase of $Na_2B_{12}H_{12}$. X-ray and neutron diffraction studies indicate that this latter phase is comprised of a body-centered-cubic arrangement of orientationally disordered $[B_{12}H_{12}]^{2-}$ anions with crystallographically disordered Na^+ cations occupying an array of off-center positions within the distorted tetrahedral interstices. The structural behavior of this phase transition will be published in fuller detail elsewhere. Since at the high-temperature slope of the relaxation rate peak, R_1^H is proportional to τ, the observed sharp decrease in R_1^H corresponds to a nearly 2 orders of magnitude *increase* in the reorientation jump rate τ^{-1} in the high-temperature phase. Similar behavior of R_1^H was observed at the tetragonal-to-cubic phase transition in $NaBH_4$,[15] although, in the case of the borohydride, the drop in R_1^H was much smaller (by about 1 order of magnitude). It should be noted that the ^{1}H NMR line width does not show any significant changes near the phase transition point in $Na_2B_{12}H_{12}$; the value of $\Delta\nu_H$ remains to be nearly constant (~10 kHz) in the range 450−570 K. This indicates that the behavior of the ^{1}H NMR parameters in both phases is governed by localized H motion, so that even strong changes in τ^{-1} do not affect the plateau value of $\Delta\nu_H$. In the studied temperature range, we have not found any signs of translational diffusion of H-containing species on the frequency scale of 10^5 s^{-1}. For the high-temperature phase of $Na_2B_{12}H_{12}$, the activation energy for reorientations estimated from the slope of the log R_1^H vs T^{-1} plot (Figure 7) is 270 ± 40 meV. This value is nearly 3 times lower than that for the low-temperature phase of the same compound; such a low value of E_a is consistent with the fast reorientational motion in the high-T phase. The activation energies for both the low-T and high-T phases of $Na_2B_{12}H_{12}$ derived from the $R_1^H(T)$ data are included in Table 1. It should be noted that while the activation energy of reorientations in the high-T phase can be obtained from the temperature dependence of R_1^H, the absence of the relaxation rate peak for this phase does not allow us to determine the absolute values of τ^{-1} accurately. In Figure 4, the approximate character of τ^{-1} values for the high-T phase of $Na_2B_{12}H_{12}$ is reflected by the green shaded area.

Figure 8 shows the behavior of the ^{11}B spin−lattice relaxation rate for $Na_2B_{12}H_{12}$ measured at two resonance frequencies. It

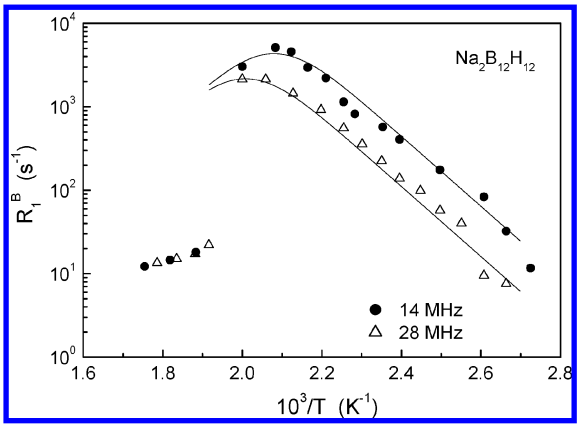

Figure 8. ^{11}B spin−lattice relaxation rates measured at 14 and 28 MHz for $Na_2B_{12}H_{12}$ as functions of the inverse temperature. The solid lines show the simultaneous fits of the model based on eqs 2 and 1 to the data for the low-temperature phase.

can be seen that general features of the temperature dependence of R_1^B are similar to those of R_1^H (Figure 7). In particular, there is a 2 orders of magnitude drop in R_1^B near 520 K, and at T > 520 K the ^{11}B spin−lattice relaxation rate exhibits a weak temperature dependence being frequency-independent. These results support our conclusion that the transition from the low-T monoclinic to the high-T cubic phase of $Na_2B_{12}H_{12}$ is accompanied by the nearly 2 orders of magnitude increase in the reorientational jump rate. For the low-T phase, the simultaneous fit of the model based on eqs 2 and 1 to the $R_1^B(T)$ data at two frequencies gives $\tau_0 = (7.9 \pm 2.3) \times 10^{-17}$ s and E_a = 770 ± 20 meV. These values of the motional parameters are very close to the corresponding values derived from the proton spin−lattice relaxation data. The results of this fit are shown by solid lines in Figure 8. For the high-T phase of $Na_2B_{12}H_{12}$, the activation energy for reorientations estimated from the slope of the log R_1^B vs T^{-1} plot (Figure 8) is 280 ± 40 meV, in agreement with the corresponding value obtained from the $R_1^H(T)$ data.

The onset of rapid $[B_{12}H_{12}]^{2-}$ reorientations concomitant with the highly disordered nature of the interstitial Na^+ cations upon transformation to the high-temperature structure suggests that conditions are favorable for a profound enhancement in Na^+ translational mobility. In order to probe the changes in cation mobility near the phase transition point in $Na_2B_{12}H_{12}$, we have measured the ^{23}Na NMR spectra and spin−lattice relaxation rates at $\omega/2\pi$ = 23 MHz over the temperature range 458−580 K. Figure 9 shows the shapes of the ^{23}Na NMR spectra at three temperatures. At T < 520 K, the observed shapes suggest that the quadrupole interaction is not fully

dx.doi.org/10.1021/jp4106585 | J. Phys. Chem. C 2013, 117, 25961−25968

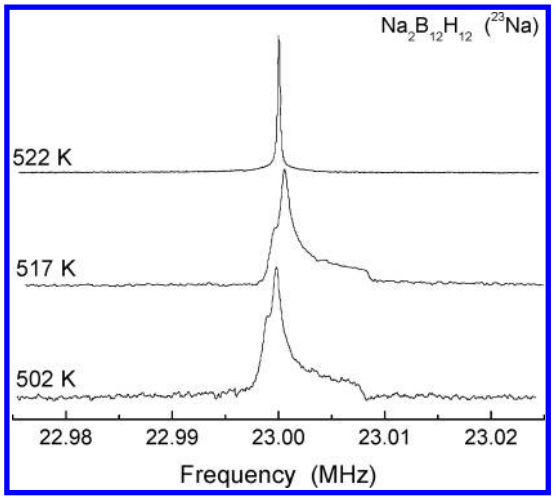

Figure 9. ^{23}Na NMR line shapes for $Na_2B_{12}H_{12}$ below and above the phase transition point.

averaged out by atomic motion. Above the phase transition point, the ^{23}Na NMR line becomes symmetric and very narrow.

The behavior of the ^{23}Na NMR line width (full width at half-maximum) is shown in Figure 10. Such a behavior indicates

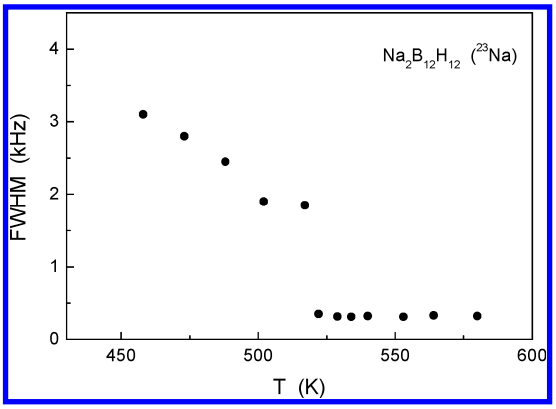

Figure 10. Temperature dependence of the width (full width at half-maximum) of the ^{23}Na NMR line for $Na_2B_{12}H_{12}$.

that above the phase transition point both the quadrupole and dipole−dipole interactions of ^{23}Na nuclei are averaged out. In fact, the observed ^{23}Na NMR line width in the high-temperature phase (0.31 kHz) is considerably smaller than the expected line width (~0.96 kHz) for the ^{23}Na−^{23}Na dipolar contribution to the rigid lattice second moment. This can occur only in the case of translational diffusion of Na ions.

Therefore, we can conclude that the phase transition from the monoclinic to the cubic phase of $Na_2B_{12}H_{12}$ is accompanied by the onset of translational Na^+ diffusion with the jump rate exceeding ~10^5 s^{-1}. Similar behavior of the cation translational mobility was observed near the temperature of the first-order phase transition in $LiBH_4$.[17,24−26] As we shall discuss below, on the basis of the ^{23}Na spin−lattice relaxation measurements, the estimated lower limit of the Na^+ jump rate in the cubic phase can be pushed to much higher values.

The behavior of the measured ^{23}Na spin−lattice relaxation rate R_1^{Na} near the phase transition point in $Na_2B_{12}H_{12}$ is shown in Figure 11. As can be seen from this figure, the phase transition is accompanied by the jump in the ^{23}Na relaxation rate and by the change of the sign of its temperature

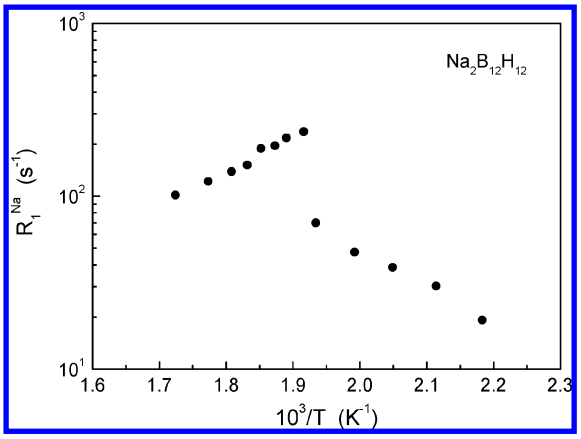

Figure 11. ^{23}Na spin−lattice relaxation rate measured at 23 MHz for $Na_2B_{12}H_{12}$ as a function of the inverse temperature.

dependence. In terms of the motionally induced spin−lattice relaxation, such a behavior can be described as "folding" of the relaxation rate peak:[27] due to the abrupt change in the atomic jump rate at the phase transition, the relaxation rate jumps directly from the low-temperature slope of the peak to its high-temperature slope.

It should be noted that the measured values of R_1^{Na} near the phase transition are much higher than those expected for the ^{23}Na−^{1}H dipole−dipole interaction. Indeed, the estimate of the ^{23}Na−^{1}H contribution to the rigid-lattice second moment of ^{23}Na NMR line on the basis of the structural data[10] gives 2.9 × 10^8 s^{-2}. The full modulation of this ^{23}Na−^{1}H interaction due to Na diffusion would result in the maximum ^{23}Na spin−lattice relaxation rate value of 1.9 s^{-1} at 23 MHz. The measured R_1^{Na} values are much higher (up to 236 s^{-1}); therefore, the ^{23}Na spin−lattice relaxation is dominated by the quadrupole contribution. Furthermore, the behavior of $R_1^{Na}(T)$ in the high-temperature phase should be governed by translational Na^+ diffusion with the jump rate τ_d^{-1}. In fact, the reorientational jump rate τ^{-1} of $[B_{12}H_{12}]^{2-}$ anions above the phase transition point is of the order of 10^{11} s^{-1} (see Figure 4), i.e., much higher than the resonance frequency ω. Such a fast jump process cannot give a significant contribution to the ^{23}Na spin−lattice relaxation rate. On the other hand, the observed behavior of $R_1^{Na}(T)$ is consistent with the slower process of Na^+ diffusion with τ_d^{-1} slightly exceeding ω just above the transition point. Thus, the lower limit of the Na^+ jump rate in the high-T phase can be estimated as 2 × 10^8 s^{-1}. The activation energy $E_a{}^d$ for Na^+ diffusion derived from the slope of the log R_1^{Na} vs T^{-1} plot for the high-T phase (Figure 11) is 410 ± 25 meV. Note that this value is considerably higher than the activation energy E_a for anion reorientations in the high-T phase. Such a difference supports our conclusion that the behavior of $R_1^{Na}(T)$ above the phase transition point is governed by translational diffusion of Na ions.

CONCLUSIONS

The analysis of the temperature and frequency dependences of the measured ^{1}H and ^{11}B spin−lattice relaxation rates for cubic $K_2B_{12}H_{12}$, $Rb_2B_{12}H_{12}$, and $Cs_2B_{12}H_{12}$ has shown that for all these compounds the relaxation data are governed by thermally activated reorientations of the icosahedral $[B_{12}H_{12}]^{2-}$ anions. The jump rates τ^{-1} of this reorientational motion derived from our data are found to change by 4−5 orders of magnitude over

dx.doi.org/10.1021/jp4106585 | J. Phys. Chem. C 2013, 117, 25961−25968

the studied temperature range of 250−570 K. The activation energies E_a for the reorientational motion decrease with increasing cation radius (and increasing lattice parameter); the values of E_a obtained from our proton spin−lattice relaxation data are 800 ± 8 meV for $K_2B_{12}H_{12}$, 549 ± 5 meV for $Rb_2B_{12}H_{12}$, and 427 ± 4 meV for $Cs_2B_{12}H_{12}$. In the studied temperature range, we have not found any signs of distributions of the jump rates for the reorientational motion.

For monoclinic $Na_2B_{12}H_{12}$ (T < 520 K), the behavior of the measured ^1H and ^{11}B spin−lattice relaxation rates is also governed by thermally activated reorientations of $[B_{12}H_{12}]^{2-}$ anions with E_a = 770 ± 20 meV. It is found that the first-order transition from the low-T monoclinic to the high-T cubic phase of $Na_2B_{12}H_{12}$ near 520 K is accompanied by a 2 orders of magnitude increase in the reorientational jump rate τ^{-1}. Just above the transition point, the values of τ^{-1} are of the order of 10^{11} s^{-1}, and the temperature dependence of τ^{-1} is described by the low activation energy (~270 meV). Our measurements of the ^{23}Na NMR spectra and spin−lattice relaxation rates indicate that the transition from the low-T to the high-T phase is also accompanied by the onset of the fast translational diffusion of Na^+ ions. Just above the transition point, the lower limit of the jump rate τ_d^{-1} for Na^+ diffusion estimated from the ^{23}Na spin−lattice relaxation data is 2 × 10^8 s^{-1}, and the corresponding activation energy E_a^d is ~410 meV. This is the first evidence for fast cation diffusion in $B_{12}H_{12}$-based compounds. It is interesting that the jump in Na^+ mobility is concomitant with the jump in the reorientational rate of $[B_{12}H_{12}]^{2-}$ anions. To what extent the anion dynamical changes aid the enhanced cation mobility is yet to be determined.

AUTHOR INFORMATION

Corresponding Author

*E-mail skripov@imp.uran.ru; Fax +7-343-374-5244.

Notes

The authors declare no competing financial interest.

ACKNOWLEDGMENTS

This work was supported by the U.S. Department of Energy EERE (Grants DE-EE0002978, DE-AI-01-05EE11104, and DE-AC04-94AL85000), the Russian Foundation for Basic Research (Grant 12-03-00078), the Priority Program 12-P-2-1050 "Physico-technical principles of development of technologies and devices for smart adaptive electrical networks" of the Russian Academy of Sciences (RAS), and the collaborative Grant RUP1-7076-EK-12 from the Ural Branch of RAS and the U.S. Civilian Research & Development Foundation (CRDF Global) with funding from the U.S. Department of State. The opinions, findings and conclusions stated herein are those of the authors and do not necessarily reflect those of CRDF Global or the U.S. Department of State.

REFERENCES

(1) Verdal, N.; Wu, H.; Udovic, T. J.; Stavila, V.; Zhou, W.; Rush, J. J. Evidence of a Transition to Reorientational Disorder in the Cubic Alkali-Metal Dodecahydro-*closo*-Dodecaborates. *J. Solid State Chem.* **2011**, *184*, 3110−3116.

(2) Pitt, M. P.; Paskevicius, M.; Brown, D. H.; Sheppard, D. A.; Buckley, C. E. Thermal Stability of $Li_2B_{12}H_{12}$ and Its Role in the Decomposition of $LiBH_4$. *J. Am. Chem. Soc.* **2013**, *135*, 6930−6941.

(3) Paskevicius, M.; Pitt, M. P.; Brown, D. H.; Sheppard, D. A.; Chumphongphan, S.; Buckley, C. E. First-Order Phase Transition in the $Li_2B_{12}H_{12}$ System. *Phys. Chem. Chem. Phys.* **2013**, *15*, 15825−15828.

(4) Orimo, S.; Nakamori, Y.; Ohba, N.; Miwa, K.; Aoki, M.; Towata, S.; Züttel, A. Experimental Studies on Intermediate Compound of $LiBH_4$. *Appl. Phys. Lett.* **2006**, *89*, 021920.

(5) Hwang, S.-J.; Bowman, R. C.; Reiter, J. W.; Rijssenbeek, J.; Soloveichik, G. L.; Zhao, J.-C.; Kabbour, H.; Ahn, C. C. NMR Confirmation for Formation of $[B_{12}H_{12}]^{2-}$ Complexes during Hydrogen Desorption from Metal Borohydrides. *J. Phys. Chem. C* **2008**, *112*, 3164−3169.

(6) Garroni, S.; Milanese, C.; Pottmaier, D.; Mulas, G.; Nolis, P.; Girella, A.; Caputo, R.; Olid, D.; Teixdor, F.; Baricco, M.; et al. Experimental Evidence of $Na_2[B_{12}H_{12}]$ and Na Formation in the Desorption Pathway of the $2NaBH_4 + MgH_2$ System. *J. Phys. Chem. C* **2011**, *115*, 16664−16671.

(7) Kim, K. C.; Sholl, D. S. Crystal Structures and Thermodynamic Investigations of $LiK(BH_4)_2$, KBH_4, and $NaBH_4$ from First-Principles Calculations. *J. Phys. Chem. C* **2010**, *114*, 678−686.

(8) Tiritiris, I.; Schleid, T. Die Dodekahydro-*closo*-Dodekaborate $M_2[B_{12}H_{12}]$ der Schweren Alkalimetalle (M^+ = K^+, Rb^+, NH_4^+, Cs^+) und Ihre Formalen Iodid-Addukte $M_3I[B_{12}H_{12}]$ (≡ $MI{\times}M_2[B_{12}H_{12}]$). *Z. Anorg. Allg. Chem.* **2003**, *629*, 1390−1402.

(9) Tiritiris, I.; Schleid, T.; Müller, K.; Preetz, W. Strukturelle Untersuchungen an $Cs_2[B_{12}H_{12}]$. *Z. Anorg. Allg. Chem.* **2000**, *626*, 323−325.

(10) Her, J.-H.; Zhou, W.; Stavila, V.; Brown, C. M.; Udovic, T. J. Role of Cation Size on the Structural Behavior of the Alkali-Metal Dodecahydro-*closo*-Dodecaborates. *J. Phys. Chem. C* **2009**, *113*, 11187−11189.

(11) Her, J.-H.; Yousufuddin, M.; Zhou, W.; Jalisatgi, S. S.; Kulleck, J. G.; Zan, J. A.; Hwang, S.-J.; Bowman, R. C.; Udovic, T. J. Crystal Structure of $Li_2B_{12}H_{12}$: a Possible Intermediate Species in the Decomposition of $LiBH_4$. *Inorg. Chem.* **2008**, *47*, 9757−9759.

(12) Tiritiris, I.; Schleid, T.; Müller, K. Solid-State NMR Studies on Ionic *closo*-Dodecaborates. *Appl. Magn. Reson.* **2007**, *32*, 459−481.

(13) Verdal, N.; Udovic, T. J.; Rush, J. J.; Cappelletti, R. L.; Zhou, W. Reorientational Dynamics of the Dodecahydro-*closo*-dodecaborate Anion in $Cs_2B_{12}H_{12}$. *J. Phys. Chem. A* **2011**, *115*, 2933−2938.

(14) Skripov, A. V.; Soloninin, A. V.; Babanova, O. A. Nuclear Magnetic Resonance Studies of Atomic Motion in Borohydrides. *J. Alloys Compd.* **2011**, *509S*, S535−S539.

(15) Babanova, O. A.; Soloninin, A. V.; Stepanov, A. P.; Skripov, A. V.; Filinchuk, Y. Structural and Dynamical Properties of $NaBH_4$ and KBH_4: NMR and Synchrotron X-ray Diffraction Studies. *J. Phys. Chem. C* **2010**, *114*, 3712−3718.

(16) Markert, J. T.; Cotts, E. J.; Cotts, R. M. Hydrogen Diffusion in the Metallic Glass *a*-$Zr_3RhH_{3.5}$. *Phys. Rev. B* **1988**, *37*, 6446−6452.

(17) Skripov, A. V.; Soloninin, A. V.; Filinchuk, Y.; Chernyshov, D. Nuclear Magnetic Resonance Study of the Rotational Motion and the Phase Transition in $LiBH_4$. *J. Phys. Chem. C* **2008**, *112*, 18701−18705.

(18) Skripov, A. V.; Soloninin, A. V.; Babanova, O. A.; Hagemann, H.; Filinchuk, Y. Nuclear Magnetic Resonance Study of Reorientational Motion in α-$Mg(BH_4)_2$. *J. Phys. Chem. C* **2010**, *114*, 12370−12374.

(19) Stavila, V.; Her, J.-H.; Zhou, V.; Hwang, S.-J.; Kim, C.; Ottley, L. A. M.; Udovic, T. J. Probing the Structure, Stability and Hydrogen Storage Properties of Calcium Dodecahydro-*closo*-Dodecaborate. *J. Solid State Chem.* **2010**, *183*, 1133−1140.

(20) The mention of all commercial suppliers in this paper is for clarity. This does not imply our recommendation or endorsement of these suppliers.

(21) Abragam, A. *The Principles of Nuclear Magnetism*; Clarendon Press: Oxford, 1961.

(22) Babanova, O. A.; Soloninin, A. V.; Skripov, A. V.; Ravnsbæk, D. B.; Jensen, T. R.; Filinchuk, Y. Reorientational Motion in Alkali-Metal Borohydrides: NMR Data for $RbBH_4$ and $CsBH_4$ and Systematics of the Activation Energy Variations. *J. Phys. Chem. C* **2011**, *115*, 10305−10309.

(23) Cotts, R. M. Nuclear Magnetic Resonance on Metal−Hydrogen Systems. In *Hydrogen in Metals I*; Alefeld, G., Völkl, J., Eds.; Springer: Berlin, Germany, 1978; pp 227−265.
(24) Matsuo, M.; Nakamori, Y.; Orimo, S.; Maekawa, H.; Takamura, H. Lithium Superionic Conduction in Lithium Borohydride Accompanied by Structural Transition. *Appl. Phys. Lett.* **2007**, *91*, 224103.
(25) Corey, R. L.; Shane, D. T.; Bowman, R. C.; Conradi, M. S. Atomic Motions in $LiBH_4$ by NMR. *J. Phys. Chem. C* **2008**, *112*, 18706−18710.
(26) Soloninin, A. V.; Skripov, A. V.; Buzlukov, A. L.; Stepanov, A. P. Nuclear Magnetic Resonance Study of Li and H Diffusion in the High-Temperature Phase of $LiBH_4$. *J. Solid State Chem.* **2009**, *182*, 2357−2361.
(27) Skripov, A. V.; Belyaev, M.Yu.; Rychkova, S. V.; Stepanov, A. P. Nuclear Magnetic Resonance Study of Hydrogen Diffusion in $HfV_2H_x(D_x)$ and $ZrV_2H_x(D_x)$: Effects of Phase Transitions and Isotope Substitution. *J. Phys.: Condens. Matter* **1991**, *3*, 6277−6291.